T9079-D

Theory Based Process Modeling for Evaluation of Fuel Cells in Advanced Energy Systems

Rodney A. Geisbrecht
National Energy Technology Laboratory
Pittsburgh, PA 15236-0940

Prepared for presentation at the Spring 2002 National Meeting, New Orleans, LA, March 10-14
Unpublished

Abstract

The development of advanced energy systems is an important objective in DOE programs, such as the Vision 21 Program, where ambitious goals are targeted for efficiency, cost, and/or emissions, including the possibility of zero emission systems with capture and sequestration of carbon dioxide. Hybrids, in which fuel cells are combined with other power cycles, underlie many of the promising concepts. To consistently evaluate the variety of concepts, a theory based process model of fuel cells is important to account for the diverse range of conditions proposed for their application. Another important aspect to the model is its compatibility and consistency with the process simulator being used for systems analysis. This paper describes a theory based process modeling approach used at NETL, along with some examples.

Background

Of special importance is the prediction of cell voltage and current density relationships over a broad range of conditions. For the simple idealization of a coflow geometry with constant resistance, Ω, current density distribution is solely determined by the variation of Nernst potential, E, with fuel conversion, X, or the so-called Nernst potential losses:

$$i_m/i_r = \{(\int^{X_r} ((E_r - E_c) / (E - E_c))\, dX) / X_r\}^{-1}$$

where:
$i_m \equiv$ average current density
$i_r \equiv$ reference current density $= (E_r - E_c) / \Omega$

A typical Nernst potential curve for a solid oxide fuel cell (SOFC) is shown in Figure 1. A characteristic of high temperature fuel cells, the Nernst potential falls steeply at high fuel utilization, with the result that the current density distribution becomes more nonuniform as cell voltage, E_c, approaches the minimum Nernst potential, E_r, evaluated at the cell exit. Values of dimensionless average current density, a measure of this nonuniformity, are shown in Figure 2. This simple example illustrates the importance of estimating current density distributions for more complicated cases, including crossflow geometry and important idealizations that aren't well approximated by the constant resistivity assumption, such as adiabatic cells with significant heat effects. Combined with temperature dependent resistivities, it becomes possible to estimate the impact of gradients in both temperature and Nernst potential on current density. Furthermore, the local resistance

can be generalized to include the composite effects of ohmic resistance, electrocatalyst activation, and gas diffusion in porous electrodes.

Heat and Material Balances (Rating Sequence)

Table 1 summarizes the main features of the modeling methodology. It consists of two sequences of unit operation models; an initial sequence, called the rating stage, and a final sequence called the design stage. The rating sequence is used in the determination heat and material balances, and is embedded in the main flowsheet sequence wherein the fuel cell is one component among many in the balance of plant (BOP). In the rating sequence, we are thus concerned only with overall heat and material balances around the fuel cell for a specified cell voltage or voltage efficiency.

A diagram of the rating sequence for a SOFC is shown in Figure 3. An isentropic reactor is used for all high temperature fuel cells, since these are generally operated in adiabatic mode. An equlibrium model is used for calculations (Aspen RGIBBS with reforming, shifting, and oxidation reactions enabled). For a SOFC, pure O2 is exchanged from the cathode to anode stream; for a molten carbonate fuel cell (MCFC), two units of CO2 accompany each unit of O2, and fuel reforming reactions are optional. Equilibrium is generally inadequate for all aspects (it notably overpredicts actual NOX emissions, for example), but is assumed to be good enough for the reactions that control heat and material balances and current density distributions.

An isothermal, reversible reactor is used for low temperature fuel cells, since these generally have a heat exchanger integrated into the stack. A restricted equilibrium model is used for the calculations (Aspen RGIBBS with shifting and hydrogen oxidation enabled). For both a phosphoric acid fuel cell (PAFC) and a polymer electrolyte membrane fuel cell (PEMFC), H2 is exchanged from the anode stream to the cathode stream. Shifting is disallowed in PEMFC's, irrespective of the fact that CO levels are generally held to very low levels anyway in view of their adverse impact on PEMFC's.

Current Density Distribution (Design Sequence)

After flowsheet convergence, the design sequence is executed one time to determine the current density distribution. A diagram of the stand-alone design sequence is shown in Figure 4. Converged results from the rating sequence (fuel and air feeds including recycle, fuel conversion, cell voltage, heat loss, etc.) are used as input, and the same kinds of models and physical properties packages used in the rating stage are used for consistency. An outer iteration (Aspen DESIGN SPEC) is used to determine cell area, and an inner loop (Aspen Fortran Tear Variable) is used to cycle through the discretized cell. Calculation blocks (Aspen FORTRAN) are used to store fuel and air stream vectors and to determine current in each element that equilibrates the local Nernst potential to the cell voltage using cell area and local resistance. A typical result for cell voltage, as a function of IR loss at constant fuel utilization (Nernst potential loss), is shown in Figure 5. Cell voltage deviates from the hypothetical limit for staged cells below a threshold value of IR that is comparable to the IR values targeted for practical applications.

Benchmark Coflow Cases

Comparison of the SOFC model in coflow geometry to published data for tubular technology is shown in Figure 6. The data are matched well by using a network equivalent cell resistance derived from data for the older porous support tube technology (Kinoshita, 1988), as summarized in Table 2. The equivalent cell resistance refers to a discrete calculation of current density distribution, or path, around the circumference of the tube, as illustrated by Haynes and Wepfer (1996). Predicted voltages are shifted slightly higher for the newer air electrode supported technology (Singhal, 1996), and predicted power densities are within 15 percent on the high side of quoted values (Veyo and Lundberg, 1996).

Comparison of the PEMFC model in coflow geometry to published data is summarized in Figure 7. The correlation curve refers to a semi-empirical model, based on that published by Amphlett et al. (1995) which was fitted to data from Ballard's Mark IV prototype. Agreement is best in the lower current density ranges where gas diffusion overpotentials are less. The estimated resistance, derived from extrapolated VI curves, is generally consistent with membrane resistivity and thickness (Fuel Cells Handbook, 1994), if allowances are made for resistances in electrodes and current collectors, as shown in Table 3. The major uncertainties would appear to be electrocatalyst activation parameters such as the exchange current density, which could depend upon catalyst loading and preparation techniques. A value 10-fold greater than a reported value at a Pt loading of 0.15 mg/cm^2 (Fischer and Wendt, 1996) was used, since loadings ranging up to 4 mg/cm^2 are more typical (Jacoby, 1999). A key uncertainty is the mitigation of poisoning by carbon monoxide below the 10 ppm level.

Conceptual Crossflow Cases

Results for a MCFC in crossflow geometry, hypothetically operated adiabatically with direct, internal reforming to equilibrium, are shown in Figure 8. Gradients in both current density and temperature occur in both the fuel and air flow directions, with maximum current density occurring at the corner where air and fuel inlets converge. An interesting aspect to this crossflow case is that the cell voltage actually exceeds the Nernst potential difference between the mixed fuel and air exhaust streams. This is not possible in coflow geometry since the mixed gas potential difference necessarily occurs at the cell exit.

Results for a planar SOFC in crossflow geometry, hypothetically operated isothermally at the adiabatic limit with reformed fuel, are shown in Figure 9 for two cases of air:fuel equivalence ratio (AFR). The results underscore the potential for crossflow to force a more uniform current density distribution by keeping the AFR near the stoichiometric limit, but at the penalty of a significant drop in average current density, which drops from 150 to 63 mA/cm^2 as AFR is reduced from 6 to 1, respectively. This makes for an interesting systems integration and optimization problem since much of the BOP (prime movers, heat exchangers, and duct work) scales directly with the air stream. An added complexity is that AFR is not an independent design variable in the typical adiabatic fuel cell design concepts, which rely on the sensible heat carrying capacity of excess air to keep cell temperatures within the acceptable operating range. AFR's on the order of 6 are typical with externally reformed fuel. Values on the order of 3 or lower are possible with internally reformed fuel, but direct internal reforming tends to be uncontrollable at SOFC conditions, resulting in excessive cooling or carbon formation at the inlet. While Siemens/Westinghouse has managed to implement indirect internal reforming for their tubular technology, adapting such an approach to planar SOFC's remains to be seen.

Systems Applications

Various fuel cell/gas turbine hybrids are being evaluated under the DOE Hybrids/Vision 21 Programs. A matrix of proposed cycle configurations is shown in Table 4, ranging from direct fired turbines (working fluid: combustion gases) to indirect fired turbines (working fluid: fresh air heat exchanged against ambient pressure combustion gases), and from fuel cells in topping cycle (fed with fresh fuel and air) to bottoming cycle (fed with vitiated air or fuel from a partial oxidation (POX) reformer). MCFC's and SOFC's in both coflow and crossflow geometries have been proposed, and have been studied in detail by developers using detailed design codes and actual performance data. The theory based process models have been generally consistent with these studies when using cell resistances appropriate to the various technologies: 0.1 to 0.5 ohm-cm^2.

Other systems are being studied which extend the basic notion of fuel cell hybrids to include a component other than a gas turbine, such as an internal combustion engine (ICE) or another fuel cell. SOFC-PEMFC hybrids show promise for combining the reforming capability of SOFC's with the cyclability of PEMFC's and their superior thermodynamics for converting syngas (Geisbrecht, 2000). ICE-SOFC hybrids promise

the rapid startup features of ICE's in combination with the superior environmental performance of SOFC's. Interestingly, both concepts offer a way to balance the thermal and carbon deposition requirements in direct partial oxidation reforming at low levels of steam injection. As shown in Figure 10, the oxygenation (fuel combustion) requirement for carbon control tends to exceed the thermal need, particularly at low reforming temperatures. The excess thermal energy that is available for extraction directly as work via an internally reforming SOFC or ICE is commensurate with the efficiencies of these devices.

References

Amphlett, J.C., Baumert, R.M., Mann, R.F., Peppley, B.A., and P.R. Roberge, "Performance Modeling of the Ballard Mark IV Solid Polymer Electrolyte Fuel Cell," J. Electrochem. Soc., Vol. 142, No. 1, January 1995.

Geisbrecht, R. A, "Compact Electrochemical Reformer Based on SOFC Technology," Vehicular Fuel Performance: Miniaturized Hydrogen Generation Technologies, G. J. Suppes (ed.), topical conference, Spring 2000 National Meeting, AIChE, Atlanta, Georgia, March 5-9, 2000.

Fischer, A. and H. Wendt, "Electrode Porosity and Effective Electrode Catalyst Activity in Electrode Membrane Assemblies (MEAs) of PEMFCs," 1996 Fuel Cell Seminar, Orlando, Florida, November 17-20, 1996.

Fuel Cells Handbook (Revision 3), DOE/METC-94/1006, U.S Department of Energy, Morgantown, West Virginia, January, 1994.

Haynes, C. and W.J.Wepfer, "High Pressure Operation of Tubular Solid Oxide Fuel Cells and Their Integration with Gas Turbines," 1996 Fuel Cell Seminar, Orlando, Florida, November 17-20, 1996.

Kinoshita, K, "Workshop on Principles of Electrochemical Engineering for Fuel Cells," Morgantown Energy Technology Center, Morgantown, West Virginia, April 5, 1988.

Singhal, S.C., "Advances in Tubular Solid Oxide Fuel Cell Technology," 1996 Fuel Cell Seminar, Orlando, Florida, November 17-20, 1996.

Veyo, S.E. and W.L. Lundberg, "Tubular SOFC and SOFC/Gas Turbine Combined Cycles – Status and Prospects," 1996 Fuel Cell Seminar, Orlando, Florida, November 17-20, 1996.

Nomenclature

E = local Nernst potential, volts
E_r = reference Nernst potential, volts
E_c = cell voltage, volts
Ω = local composite cell resistance, ohm-cm^2
i = local current density, amp/cm^2
i_m = average current density, amp/cm^2
i_r = reference current density, amp/cm^2
X = fuel conversion
X_r = reference fuel conversion

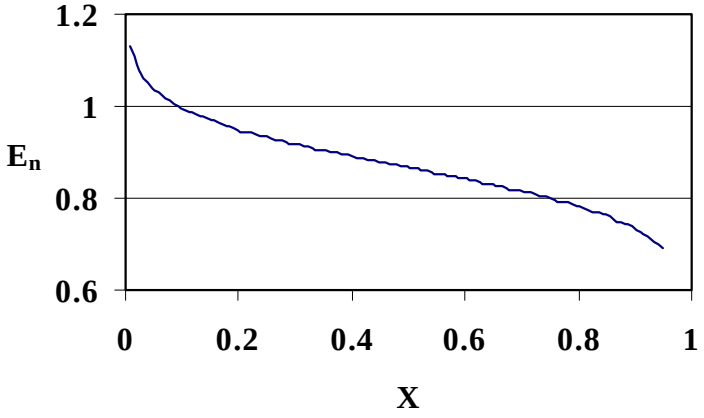

Figure 1. Nernst Potential vs Fuel Conversion in a SOFC at 1000C, 1 ATM, 1.5 Air:Fuel Equivalence Ratio – 50% Dry H2.

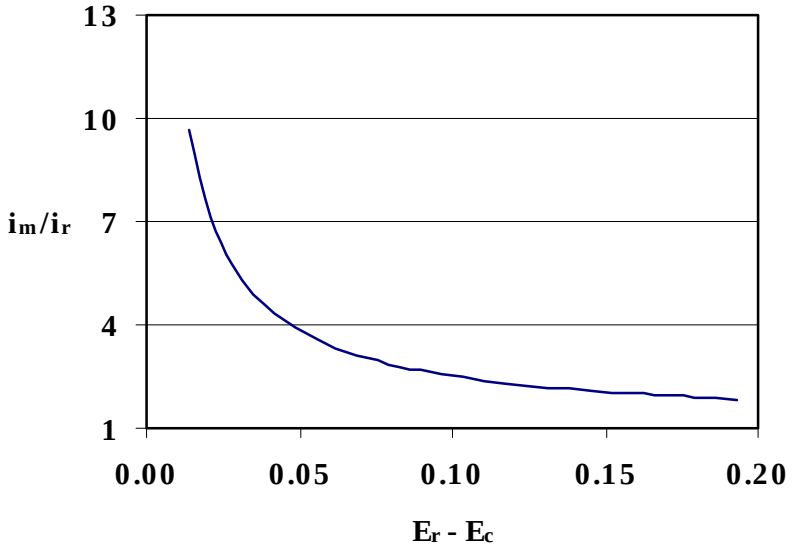

Figure 2. Index of Current Density Distribution vs E_c for Coflow with Constant Resistance and E_r Curve of Figure 1.

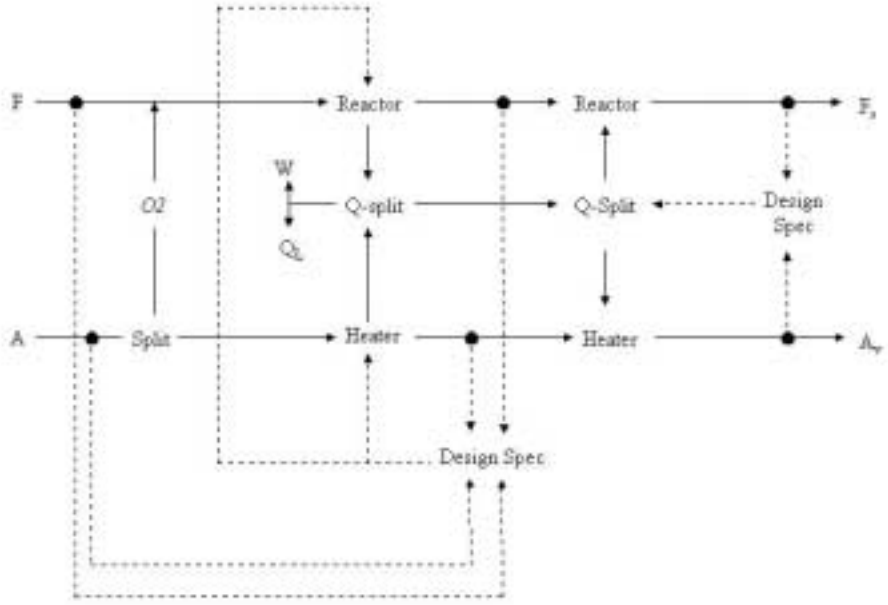

Figure 3. Rating Stage Sequence of Standard Unit Operation Models (SOFC Case)

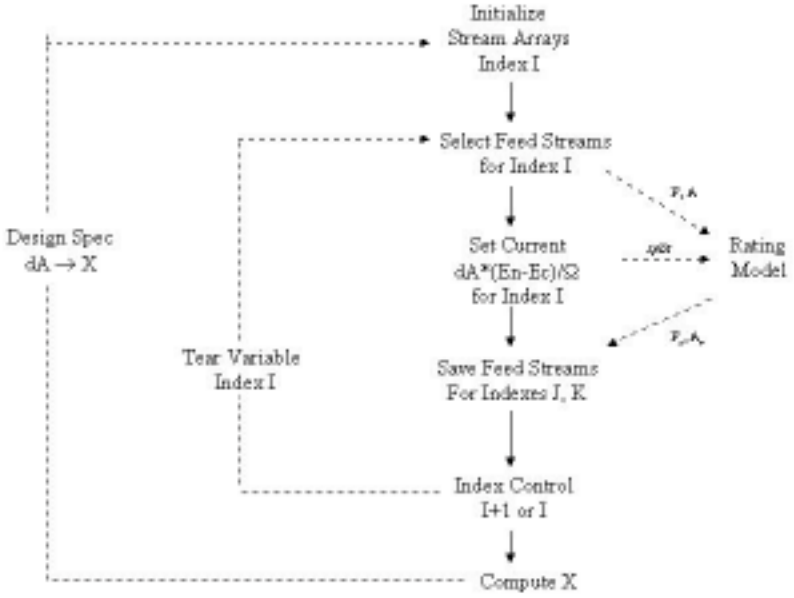

Figure 4. Design Stage Sequence for Discretized Calculations on the Flowsheet

Table 1. Process Model Sequences and Features for Fuel Cell Modeling

Model Sequences:

- **Rating stage sequence**: sequence of splitters, mixers, heaters, and reversible, restricted equilibrium reactors (adiabatic or isothermal) with cell voltage or voltage efficiency used for converging flowsheet heat and material balances.

- **Design stage sequence**: discretized version of the corresponding rating stage sequence for computing current density distributions in various geometries.

Features:

- coflow, counterflow, or crossflow manifolding
- anode gas recycle with respect to carbon deposition
- reforming and shift reaction kinetics and thermodynamics
- internal recuperation → steady state temperature distribution
- external recuperation with respect to operating temperature limits
- resistivities - electrolyte, electrode, interconnect or bipolar plate…*f*(temperature)
- activation parameters (Tafel) and gas diffusion resistances (limiting current density)

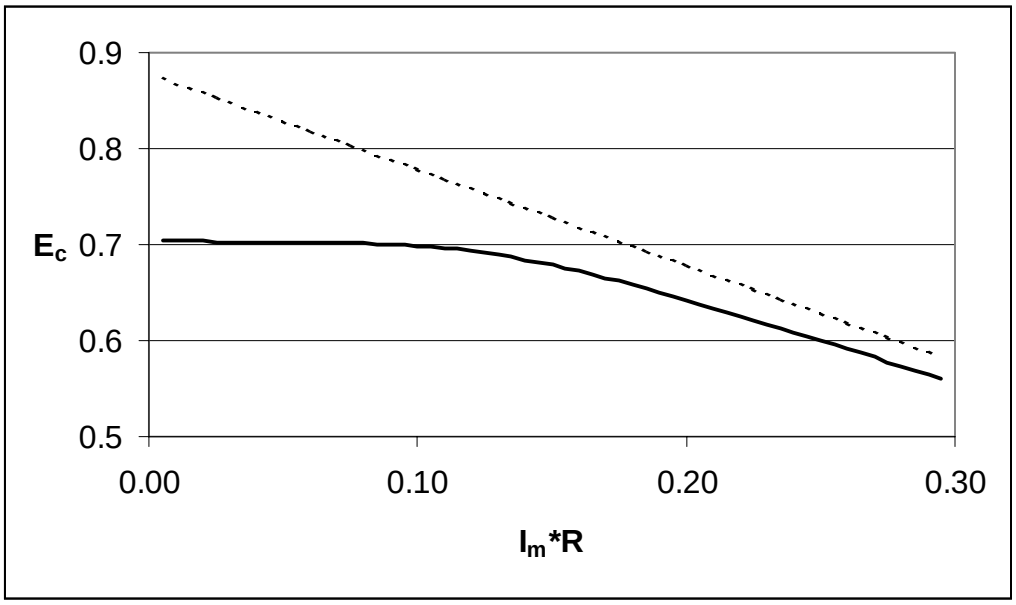

Figure 5. Typical Model Prediction with Large Nernst Potential Losses: E_c vs "IR" Product for Co-flow SOFC @ 1000C/1ATM/Dry H2/2.5 AFR/95% Fuel Conversion.

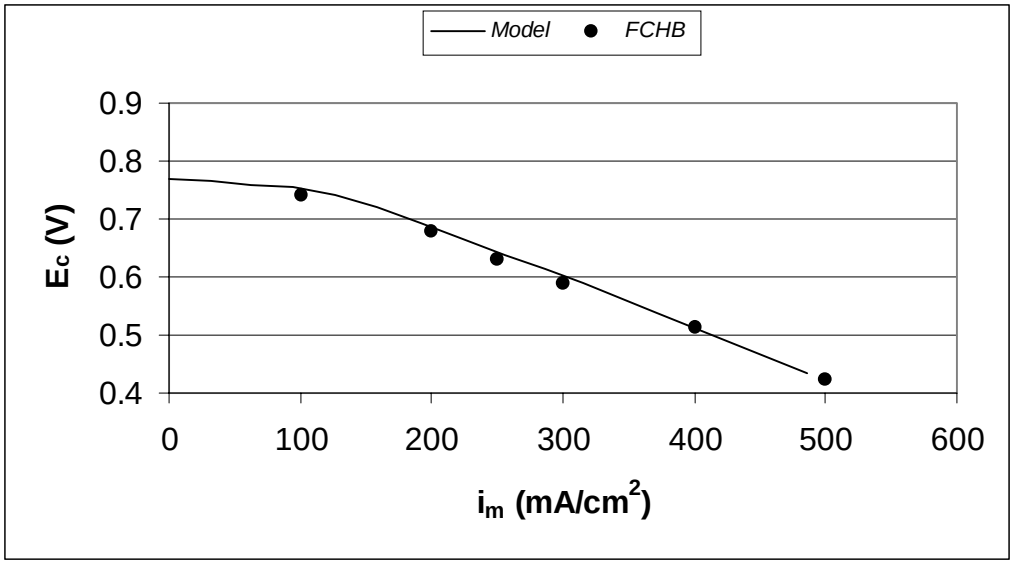

Figure 6. Tubular SOFC Performance per FCHB, Fig. 5-11 at 1000C, 85% Fuel Utilization and 25% Air Utilization. Fuel (67% H2/22% CO/11% H2O).

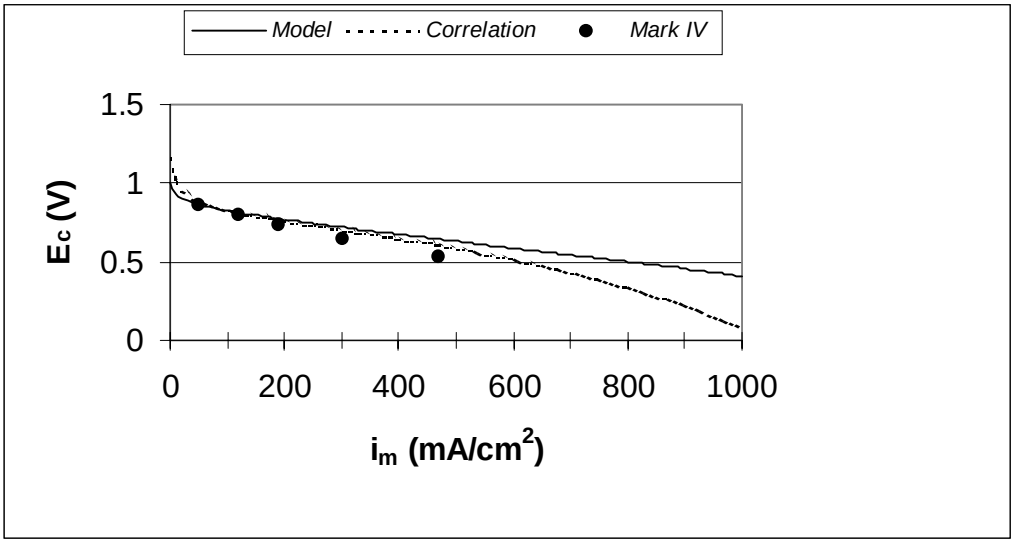

Figure 7. PEMFC Performance per Mark IV (Amphlett et al., 1995) for H2/ and Air at 70 C and 3 Atm.

Table 2. SOFC Model Parameters

Component Dimensions	**PST (Kinoshita, 1988)**	**AES (Singhal, 1998)**
cathode thickness, cm	0.07	0.22
anode thickness, cm	0.01	0.01
electrolyte thickness, cm	0.04	0.004
interconnect thickness, cm	0.04	0.0085
tube diameter, cm	1.27	2.2
interconnect chord length, cm	0.60	0.6 (estimated)
Resistivities	**Derived from Kinoshita, 1988**	**Reference @ 1000C (FCHB)**
cathode, ohm-cm	Exp(-5.48+1210/(T+273.))	0.013
interconnect, ohm-cm	Exp(-4.51+4770/(T+273.))	0.5
anode, ohm-cm	Exp(-6.03-1100/(T+273.))	0.001
electrolyte, ohm-cm	Exp(-6.01+10510/(T+273.))	10
Computed Network Equivalent Cell Resistance @ 1000C		
ohm-cm^2	0.92	0.6

Table 3. PEMFC Model Parameters

Resistivities		
apparent cell resistivity, ohm-cm^2	0.35	derived from Fig. 6-3, FCHB for 7 mil Nafion 117
ionic resistivity, ohm-cm^2	0.19	7 mil Nafion at .09 S/cm (Jacoby, 1999)
	---	
apparent electronic resistivity, ohm-cm^2	0.16	
Activation		
Tafel slope, volts/decade	0.07	Amphlett et al.,1995
apparent exchange current density, mA/cm^2	0.04	(.0037 @ .15 mg/cm^2 Pt/C, Fischer and Wendt, 1996)
Diffusion		
limiting current density, mA/cm^2	1100	estimated/arbitrary cutoff point

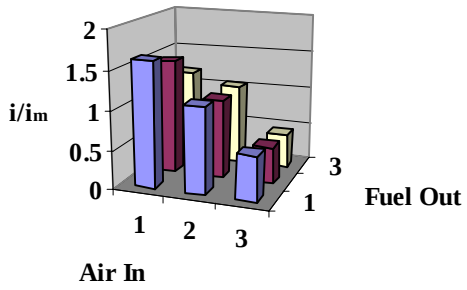

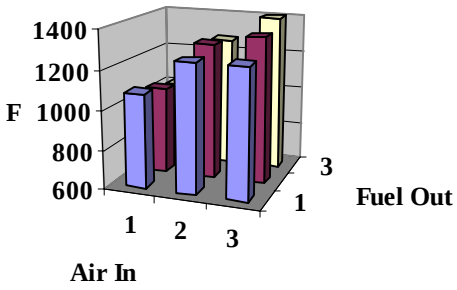

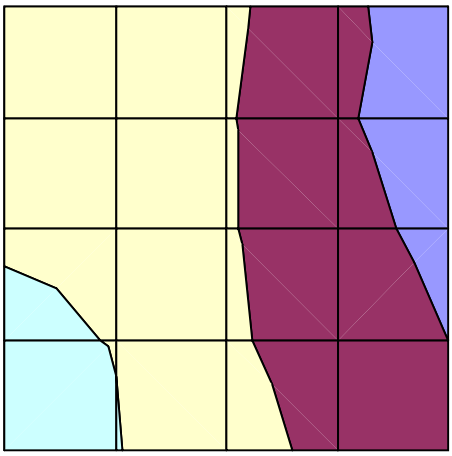

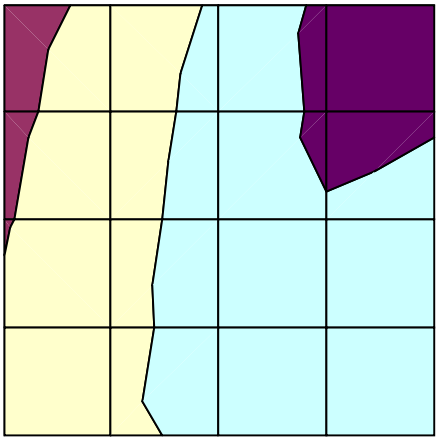

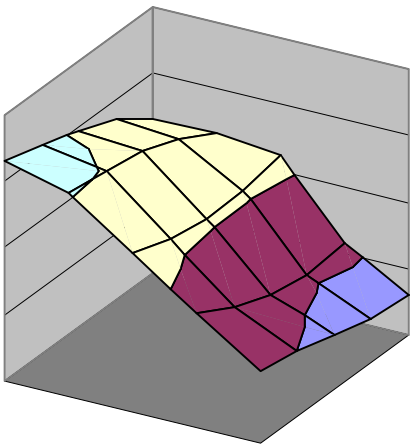

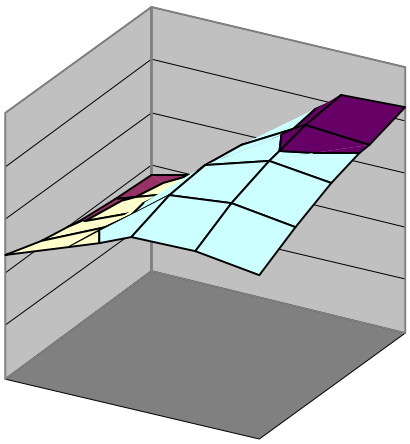

Figure 8. Current Density and Temperature Distributions for MCFC in Crossflow Geometry with Adiabatic, Direct Internal Reforming to Equilibrium.

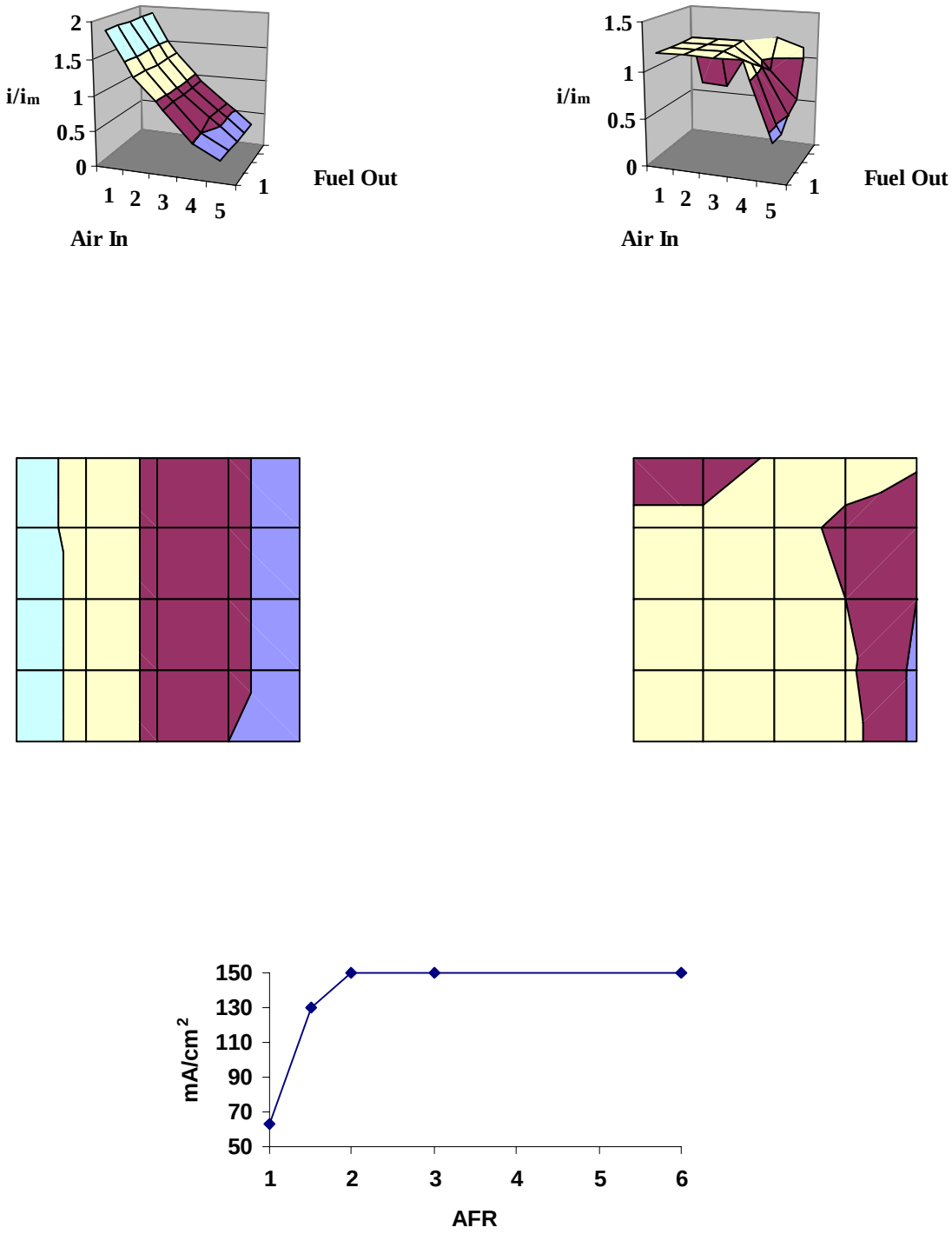

Figure 9. Current Density Distribution vs Air-Fuel Equivalence Ratio for SOFC in Crossflow Geometry Operated Isothermally at 1000 C on Reformed Fuel at Constant Cell Voltage and Fuel Utilization.

Table 4. Fuel Cell/Heat Engine Cycles in Hybrid Systems (excluding bottoming steam cycles).

	Fuel Cell Cycle (fuel side)		Heat Engine Firing	
	Topping	**Bottoming**	**Direct**	**Indirect**
Hybrids/V21 Programs				
SW	SOFC	-	GT	-
MTI	SOFC	-	-	GT
HW	SOFC	-	-	GT
MCP	MCFC	-	GT	-
FCE	MCFC	-	-	GT
Other Concepts				
SOFC-PEMFC	SOFC	PEMFC	-	-
POXHE-SOFC	-	SOFC	GT/ICE	-

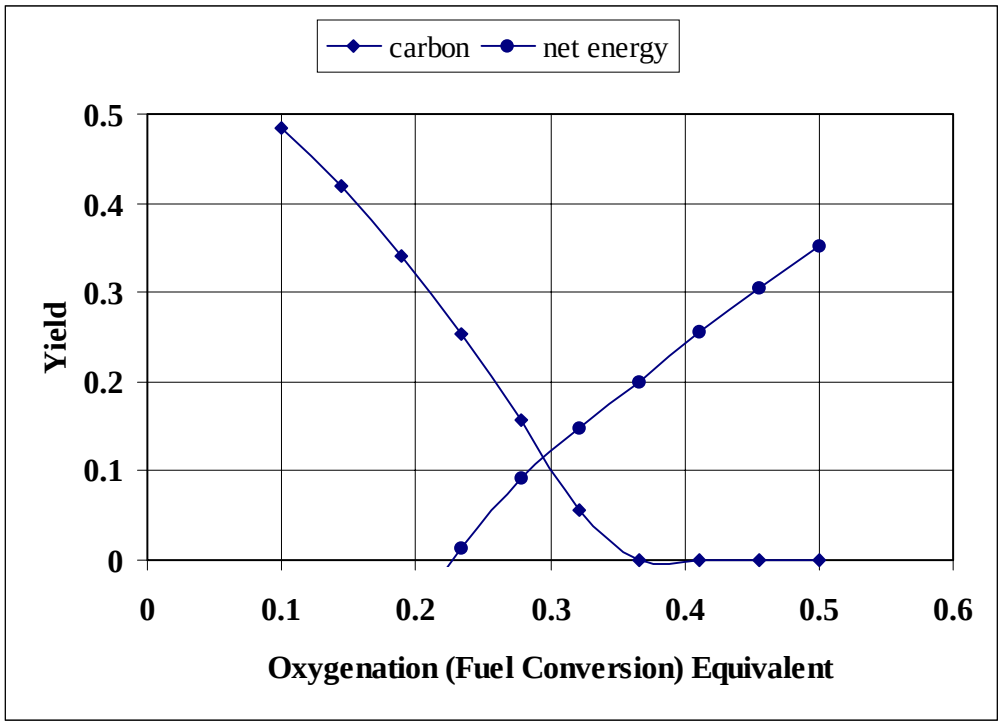

Figure 10. Carbon Yield and Excess Energy Release at Equilibrium for Direct POX Reforming of CH4 with Dry Air at 1400 F and 10 ATM.